Direct Observation of Symmetry-Breaking Trimerization in Epitaxial FeSn Kagome Films

Abstract

The Kagome lattice has attracted significant research interest due to its geometric frustration and potential for hosting topological phases. In this study, epitaxial FeSn films with alternating Kagome and honeycomb layers were grown by molecular beam epitaxy on STO(111) substrates. Using scanning tunneling microscopy and spectroscopy, a trimerization of the Fe_3Sn Kagome lattice was observed, breaking its six-fold rotational symmetry. This is evidenced by an energy-dependent reversal of high/low contrast between adjacent triangles. The trimerized structure also exhibits stripe modulations that can be tuned by an applied in-plane magnetic field. Density functional theory calculations support the assignment of Sn and Fe_3Sn terminations. The symmetry-breaking is proposed to originate from charge or bond ordering driven by coupling between the Kagome and honeycomb layers. Stripe modulations further indicate entanglement of magnetic and charge degrees of freedom. This work provides insights into electronic ordering phenomena arising from interactions and frustration in the epitaxial Kagome magnet FeSn, opening avenues for exploring topological states in layered correlated electron systems.

Introduction

The Kagome lattice is a fascinating geometric arrangement of atoms that has attracted considerable attention in the field of condensed matter physics. One of the key features of the Kagome lattice is its geometric frustration. In a regular lattice, atoms are arranged in a way that minimizes their energy, resulting in a stable configuration. However, in the Kagome lattice, the arrangement of atoms prevents them from achieving this low-energy state, leading to frustration. This frustration gives rise to exotic phenomena, such as spin liquids, where the atomic spins do not order themselves into a conventional magnetic pattern. Furthermore, the Kagome lattice has been explored in the context of topological physics, where the electronic properties of materials are governed by their topology rather than their chemical composition. By introducing certain types of interactions or external fields, researchers have been able to induce topological phases in Kagome lattice systems, such as quantum spin Hall states or topological superconductivity.

The band structure of Kagome lattice exhibits linearly dispersing Dirac cones at the Brillouin zone (BZ) corner K point and flat band (FB) through the rest of the BZ (Fig. 1b). These bands have been observed by angle-resolved photoemission spectroscopy (ARPES) in binary Kagome metal magnets T_mX_n (T: 3*d* transition metals, X: Sn, Ge, m:n=3:1, 3:2, 1:1), and ternary ferromagnetic YMn_6Sn_6. The band structure of Kagome lattice also exhibits saddle points at the BZ boundary M, which can lead to charge instabilities and symmetru-breaking electronic orders, including charge density waves (CDWs), bond order waves (BOWs), and chiral superconductivity.

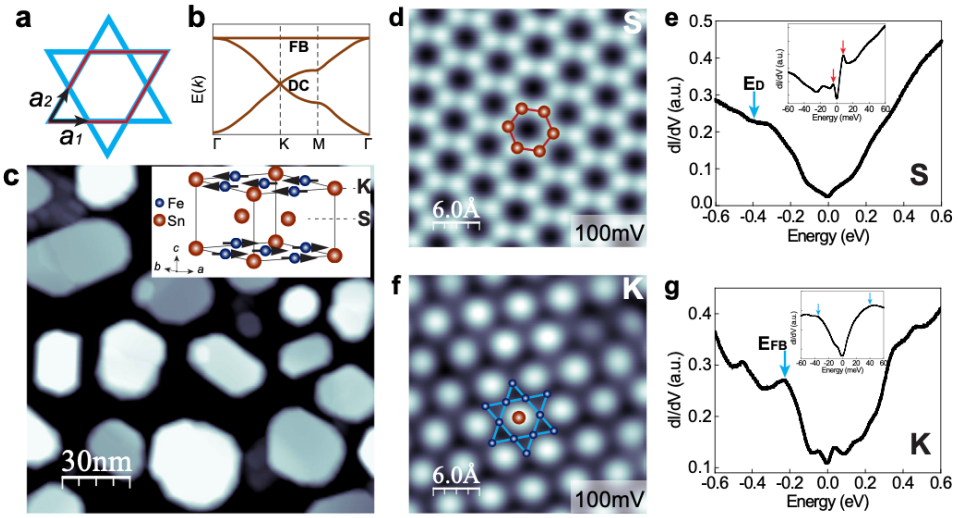

Fig. 1 FeSn films grown by MBE on the $SrTiO_3$(111) substrate with both Sn_2- and Fe_3Sn-terminations. a Model of a 2D Kagome lattice unit cell. **b** Schematic diagram of the tight binding band structure for Kagome lattice. **c** Topographic STM image of epitaxial FeSn films. Setpoint: V=5.0V, I=5pA. Inset: schematic crystal structure of FeSn with the Fe_3Sn Kagome layer (K) and Sn honeycomb layer (S) marked. **d** Atomic resolution STM image of the S layer exhibiting a honeycomb lattice. Setpoint: V=0.2V, I=3.0nA. **e** Typical dI/dV spectrum of the S layer. The cyan arrow marks the Dirac point E_D=-0.36eV. Inset: close-up view of an asymmetric gap near EF, bounded by two peaks with different intensities and energy positions at -4.0 and 7.8meV (red arrows). **f** Atomic resolution STM image of the K layer showing a close-packed lattice. Setpoint: V=0.1V, I=3.0nA. **g** Typical dI/dV spectrum of the K layer taken at the Sn site. The cyan arrow marks the flat band E_{FB}=-0.23eV. Inset: a gap of about 80meV is observed close to the Fermi level.

Here the author reports symmetry-breaking nematicity in a model Kagome magnet FeSn from the entangled magnetic and charge degrees of freedom. The crystal structure of FeSn (lattice constant a=5.3Å, c=4.4Å) is layered, consisting of alternatingly stacked planes of two-dimensional (2D) Fe_3Sn Kagome (K layer) and Sn_2 honeycomb (S layer) (Fig. 1c inset). The material is also magnetically ordered, with Fe moments ferromagnetically aligned in the K layer and antiferromagnetically coupled between K layers with Neel temperature T_N = 368K. On the epitaxy FeSn films grown on STO(111) substrates by molecular beam epitaxy (MBE), we observe a honeycomb lattice on the Sn-termination and symmetry-breaking trimerization of the Kagome lattice on the Fe_3Sn layer using scanning tunneling microscopy/spectroscopy (STM/S). This trimerized structure shows an energy-dependent high/low contrast reversal of adjacent triangles of the Kagome lattice. Furthermore, the trimerized Kagome lattice also exhibits stripe modulations that are energy-dependent and tunable by an applied in-plane magnetic field, indicating symmetry-breaking nematicity from the interplay of magnetic and charge degrees of freedom in antiferromagnet FeSe.

Data analysis

Epitaxial growth and XRD of FeSn

With a lattice mismatch of 4.0% between STO(111) substrate ($a_{STO(111)}$=5.52 Å) and FeSn (a_{FeSn}=5.30 Å), three-dimensional island growth mode is observed at the initial stages. The topographic STM image in Fig. 1c reveals a surface morphology characterized by flattop islands with heights varying from 6 to 8nm and lateral sizes typically below 50nm. As the growth proceeds, smaller islands coalesce and form larger ones with lateral sizes of about 100nm. X-ray diffraction measurements

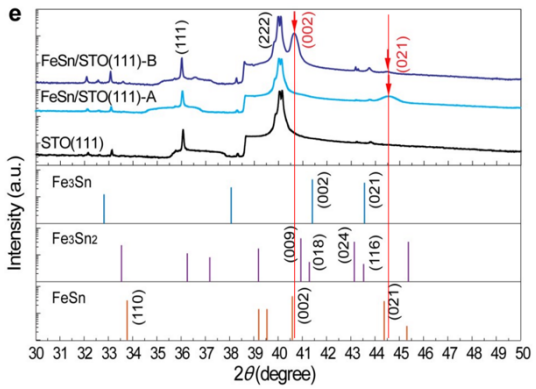

Fig. 2 X-ray diffraction of the FeSn/STO film. XRD patterns for FeSn films on STO(111) substrate. Reference data are Fe_3Sn (ICSD 24569), Fe_3Sn_2 (ICSD 71) and FeSn (ICSD 103634) from the Inorganic Crystal Structure Database.

confirm the FeSn phase (Fig 2), similar to earlier reports of MBE-grown FeSn(001) thin films on STO(111) and $LaAlO_3$(111) substrates. Comparing the XRD pattern with the references, we indicate the phase is FeSn. Note that the FeSn(002) and FeSn(021) peaks marked by the two red lines are slightly shifted to higher values, according Bragg's formular, indicating a smaller lattice constant in the *c*-direction.

STM imaging of the Sn_2-honeycomb and Fe_3Sn-Kagome layers

The Sn2 honeycomb lattice shows minimum bias dependence between ±0.5V. Figure 3a presents images taken near the Fermi level, where a uniform honeycomb is observed for all energies. This is in contrast to the surface of cleaved Fe_3Sn_2 bulk crystal, where the honeycomb structure of the Sn termination exhibits strong bias dependence, providing additional support for the FeSn film grown in this work. On the other hand, a significant bias dependence is apparent for the Fe_3Sn Kagome layer, as shown in Fig. 2b. Note that the bright contrast corresponding to the Sn atom at the center of the hexagon remains unchanged at all biases; while there is no observable difference at 100mV, the up and down Fe triangles exhibit alternating

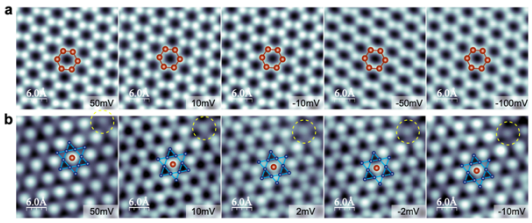

Fig. 3 Bias-dependent STM imaging of the Sn2-honeycomb (S) and Fe3Sn- Kagome (K) layers. a Atomic resolution STM images of the Sn_2-honeycomb on the Sn_2-terminated FeSn at the bias voltages specified. Setpoint: I=5.0nA. **b** Bias-dependent STM images of the Fe_3Sn Kagome layer of Fe_3Sn-termination at the bias voltages specified. In both case, ball-and-stick models of the honeycomb and the Kagome lattice are overlaid on the top. Setpoint: I=3.0nA. To account for the slight thermal draft from one image to the next, a Sn vacancy circled in (**b**) is used as a reference to assign the atomic lattice.

high and low contrast at energies close to the Fermi level (Fig. 2b). The assignment of the Sn and Fe_3Sn termination is further confirmed by density-functional theory (DFT) calculations. Some recent studies on similar systems where the central Sn/Ge atom is often not visible and appears as low contrast in the STM images. However, these prior studies are on the surface of cleaved bulk materials. Here, the samples are grown by MBE under Sn-rich conditions (Sn/Fe flux ratio >3), likely leading to a different atomic registry on the Fe_3Sn terminated surface.

Trimerization of the Fe3Sn Kagome layer

In order to examine the origin of the energy-dependent contrasts in the up and down triangles in STM imaging, the author carried out dI/dV mapping of the Fe_3Sn Kagome layer. Typical dI/dV spectra were obtained at the up-triangle site (A), down-triangle site (B) and the central Sn site (C) (Fig. 3a, b). Interestingly, the dI/dV intensities for the up- and down-triangles cross at 16.8meV (red arrow in Fig. 3b), below which A site has higher intensity. At about 100meV, the intensity of the C site is the highest. In the

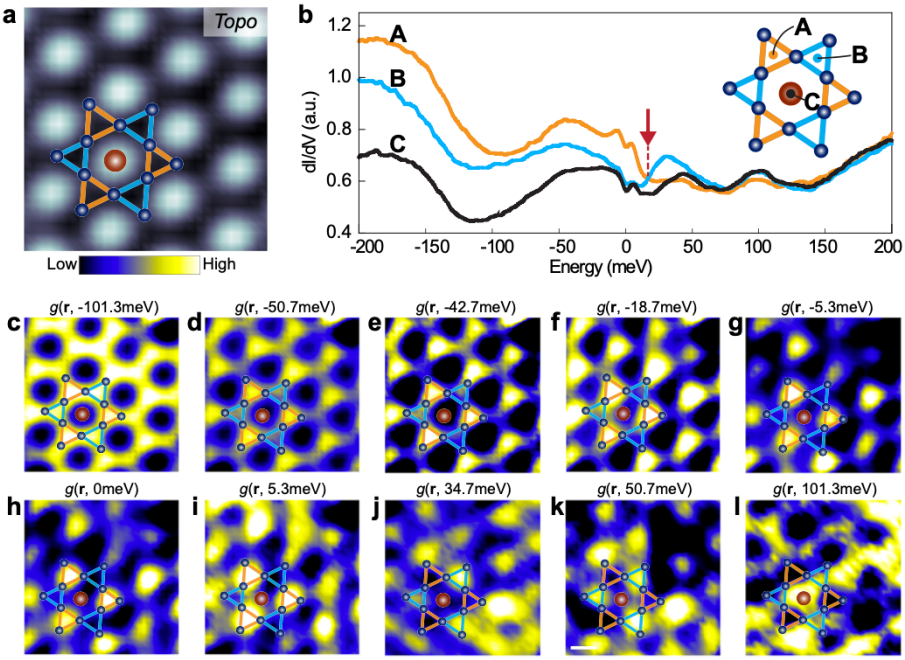

Fig. 4 Trimerized Kagome lattice on the Fe3Sn layer. a Topographic STM image of the Fe_3Sn layer. Setpoint: V=0.2 V, I=5.0nA. **b** dI/dV spectra taken at three representative sites labeled A, B, and C (inset). The red arrow marks the intensity reversal for the up-and down-triangles at 16.8meV. **c–l** Differential conductance maps of the same location at the energies marked. Setpoint: V=0.2 V, I=5.0nA. A ball-and-stick model of the Kagome lattice is overlaid on the STM image (**a**) and differential conductance maps (**c–l**).

dI/dV mapping (Fig. 4), we could also get the similar information. Below the crossing energy of 16.8meV, the up-triangles have a much higher contrast compared to the down-triangles. The contrast reverses above the transition. Around 100meV, the central Sn site has the highest contrast, while A and B sites are roughly similar. The energy-dependent contrast reversal between A and B sites indicates the trimerization of the Kagome lattice, breaking its six-fold rotational and mirror symmetry but not translational symmetry, as schematically illustrated in the inset of Fig. 4b.

Tuning the stripe modulations by an in-plane magnetic field

Since Fe atoms in the Kagome lattice are ordered ferromagnetically, the author examine the impact of the magnetic field on trimerization. Although spin-polarized tips are not used for STM imaging and spectroscopy; magnetic information cannot be obtained directly; the author still observes energy-dependent stripe modulations of the trimerized Kagome lattice.

Figure 5a shows an STM topography image and corresponding dI/dV mapping taken without magnetic field, where a close-packed structure is observed. While the close-packed structure is further confirmed by the FFT patterns shown in Fig. 5b, slight variations are present in the FFT peak intensities, indicative of a stripe modulation. By additional energy-dependent STM imaging, this is not simply due to an asymmetrical tip.

With an applied 2T in-plane magnetic field along the direction shown by the red arrow in Fig. 5c, the topography image is more symmetrical. However, the energy-dependent stripe modulations become more pronounced in the dI/dV mappings. At -144meV, the close-packed structure is modulated along one of the crystallographic directions, leading to substantially enhanced intensity at two of the peaks in the FFT pattern, as shown in second panel of Fig.

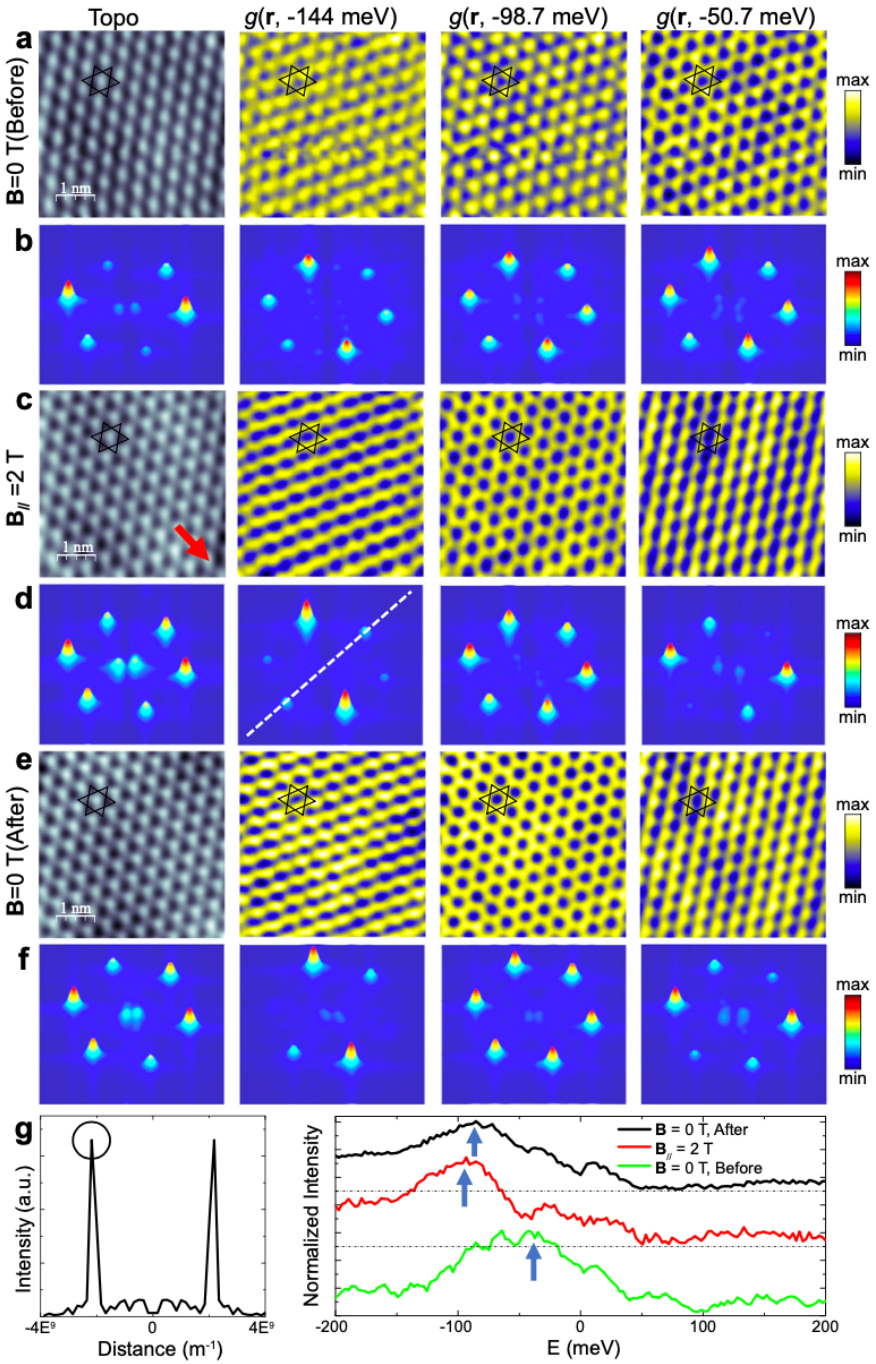

Fig. 5 Stripe modulations tunable by an in-plane magnetic field. a Topographic STM image and dI/dV maps at −144, −98.7, and −50.7meV under B = 0 T. Setpoint: V=0.2 V, I=0.7nA. **b** Patterns generated by Fast Fourier transformation (FFT) of the image and maps in (a). **c** Topographic STM image and dI/dV maps at the same energies as (a) with an in-plane magnetic field $\mathbf{B}_{//}$=2T along the direction marked by the red arrow. Setpoint: V=0.2V, I=0.7nA. **d** FFT patterns generated from the image and maps in (**c**). **e** Topographic STM image and dI/dV maps at the same energies as (a) & (c) after removing the in-plane magnetic field. Setpoint: V=0.2V, I=0.7nA. **f** FFT patterns generated from the image and maps in (**e**). **g** Left panel: line profile along the white dotted line in (**d**), with the FFT peak intensity marked by a black circle; and right panel: the energy-dependent FFT peak intensity for all the dI/dV maps at zero, 2T applied field, and after the field is removed. The curves are shifted vertically for clarity. The FFT peak intensity is normalized to their corresponding averaged background intensity.

5d. Interestingly, a honeycomb structure appears at -98.7meV, leading to a symmetrical FFT pattern. Then, the structure reverts to be close-packed at -50.7meV (right panel in Fig. 5c), but with a stripe modulation rotated 60º from that at -144meV. This stripe formation is again evident in the asymmetrical FFT patterns (Fig. 5d, right panel).

To quantify the evolution of the stripe modulation, the energy-dependent FFT peak intensity is plotted in Fig. 5g. Along the direction marked by a white dotted line in Fig. 5d second panel, the maximum peak intensity shifts from about 50meV below Fermi level at zero field to about -100meV at 2T in-plane field. Interestingly, this shift is also remanent after removing the magnetic field. However, such behavior is not observed in the other two directions, which clearly show a stripe modulation highly tunable by the magnetic field, indicating the coupling of magnetism with the charge order of the Kagome layer.

Discussion

The experimental findings reveal an intriguing trimerization of the Fe3Sn Kagome layer in epitaxial FeSn films that breaks the six-fold rotational symmetry but not the translation symmetry. One may attribute this trimerization to a breathing Kagome lattice characterized by anisotropic bond strengths with hopping parameters J_A/J_B between nearest neighbors. Such a structure is suggested for the Fe_3Sn bilayer in Fe_3Sn_2, where the two corner-sharing triangles have different bond lengths. However, the films studied here are the FeSn phase with alternatingly stacked single Sn and Fe_3Sn layers, as confirmed by the XRD data, and the observation of a perfect honeycomb without buckling on the Sn termination, in direct contrast to that observed on the Sn-terminated bulk Fe_3Sn_2. Thus, a breathing Kagome lattice in the FeSn films is unlikely.

Having ruled out the structure origin for breaking the six-fold rotational symmetry of the Kagome lattice, the author discuss electronic orders, including charge and bond orders, as other possible causes. For charge density order in non-magnetic Kagome materials, while most studies focused on the impact of the van Hove singularities at the M points, recent work highlighted the interlayer coupling of the Kagome layers where the interactions between modes at M and L points of the BZ lead to multiple CDWs, including possibly the nematic order observed in CsV_3Sb_5. In the current system of epitaxial FeSn thin film, the coupling between the Sn honeycomb layer and the Fe3Sn Kagome layer could lead to modifying the Kagome lattice. For example, if the Sn layer exhibits ($\sqrt{3}\times\sqrt{3}$) CDWs, such an order can cause different displacements of the Sn atoms underneath the neighboring triangles of the Kagome lattice, potentially leading to the trimerization. Evidence for such enhanced interlayer coupling can be found in the XRD data, where the (002) and (021) peaks of the FeSn are shifted slightly to larger values (Fig. 2) indicating a smaller *c*-axis lattice constant.

Another possible cause for breaking the six-fold rotational symmetry is the interaction-driven bond order predicted for Kagome lattices. The trimerization is consistent with several theoretically proposed bond orders and chiral flux phases. With strong bonds for the up triangles and weak bonds for the down triangles, forming such bond order waves further breaks the mirror symmetry of the Kagome lattice ad opens gaps at M points. While there haven't been reports of bond order in materials with the Kagome lattice, such order has been observed for the honeycomb lattice of graphene, where it appears as alternating high/low contrasts in STM images and dI/dV maps. Hence, the formation of bond order can also explain our observation of the

trimerization of the Kagome lattice and energy-dependent high/low contrast between adjacent triangles (Fig. 4). Such bond order is expected to open a gap, consistent with the observation of the abut 80meV gap around the E_F (Fig. 1g inset), at which the contrast reversal of neighboring triangles is also observed.

Conclusion

In conclusion, this study provides insights into symmetry-breaking electronic orders in epitaxial FeSn films with a Kagome lattice structure. STM/STS measurements reveal a trimerization of the Fe3Sn Kagome layer, breaking its six-fold rotational symmetry but not translational symmetry. This is evidenced by the energy-dependent high/low contrast reversal between adjacent triangles. The trimerization is attributed to either charge/bond order driven by interlayer coupling between the Sn honeycomb and Fe3Sn Kagome layers. Stripe modulations in the trimerized structure can be tuned by an applied in-plane magnetic field, indicating coupling between magnetic and charge degrees of freedom. This work demonstrates exotic electronic phases arising from frustration and interactions in the Kagome lattice, and sheds light on symmetry-breaking orders that could lead to topological properties in such systems. Further studies are needed to fully understand the microscopic origin and possible topological nature of the observed nematicity in epitaxial Kagome magnet FeSn films.

Methods

Samples preparation

The FeSn films were prepared by MBE with a Sn/Fe flux ratio >3 on Nb-doped (0.05 wt%) $SrTiO_3$(111) substrates. The $SrTiO_3$(111) substrates were first degassed at 600 °C for 3 h, followed by annealing at 950 °C for 1 h to obtain an atomically flat surface with step-terrace morphology. During the MBE growth, high-purity Fe (99.995%) and Se (99.9999%) were evaporated from Knudson cells on the $SrTiO_3$ substrate with temperatures between 480 and 530 °C. Annealing at high temperature, the sample could fall to the state with the lowest energy, then the atomically flat surface appears.

LT-STM/S characterization

The STM/S measurements were carried out in a low-temperature Unisoku STM system at T=4.5K. A polycrystalline Pt-Ir tip was used, which was tested on Ag/Si(111) films before the STM/S measurements. dI/dV tunneling spectra were acquired using a standard lock-in technique with a small bias modulation V_{mod} at 732 Hz. Low temperature is used to minimize the temperature drift and lock-in technique is used to minimize the environment noise.

X-ray diffraction characterization

The XRD patterns of samples were obtained using a Panalytical X'Pert Pro MPD powder X-ray diffractometer with Cu Kα X-ray source operating at 45 kV and 40 mA in the Bragg-Brentano geometry. The spectra were collected over a 2-theta range of 30° to 50° with a solid-state X-ray detector. Comparing the XRD pattern with the standard patterns, we could get the phase of the sample and analyze the change of lattice constants.

Reference

[1] Zhang, H., Oli, B.D., Zou, Q. *et al.* Visualizing symmetry-breaking electronic orders in epitaxial Kagome magnet FeSn films. *Nat Commun* **14**, 6167 (2023).